## Adsorbate vibrational mode enhancement of radiative heat transfer and van der Waals friction

A.I.Volokitin<sup>1,2\*</sup>and B.N.J.Persson<sup>1</sup>

<sup>1</sup>Institut für Festkörperforschung, Forschungszentrum Jülich, D-52425, Germany <sup>2</sup>Samara State Technical University, 443100 Samara, Russia

January 20, 2022

#### Abstract

We study the dependence of the heat transfer and the van der Waals friction between two semi-infinite solids on the dielectric properties of the bodies. We show that the heat transfer and van der Waals friction at short separation between the solids may increase by many orders of magnitude when the surfaces are covered by adsorbates, or can support low-frequency surface plasmons. In this case the heat transfer and van der Waals friction are determined by resonant photon tunneling between adsorbate vibrational modes, or surface plasmon modes. The enhancement of the van der Waals friction is especially large when in the adsorbed layer there is an acoustic branch for the vibrations parallel to the surface like in the case of Cs adsorption on Cu(100) surface. In this case we show that even for separation d = 10nm, the van der Waals friction induced by adsorbates can be so large that it can be measured with the present state-of-art equipment. The van an der Waals friction is characterized by a strong distance

<sup>\*</sup>Corresponding author: Email avoli@samgtu.ru

dependence (~  $1/d^6$ ), and at the small distances it can be much larger than the electrostatic friction observed in [9].

*Keywords*: non-contact friction, van der Waals friction, radiative heat transfer, atomic force microscope, adsorbate vibrational mode

## 1 Introduction

In the history of physics the studies of thermal radiation from materials always played a very important role. Here, it is enough to mention that quantum mechanics originated from the attempts to explain a paradoxical experimental results related to the black body radiation. In the past, the nonradiative near-field part of electromagnetic radiation usually was ignored, because it plays no role in the far-field properties of emission from planar sources. Nevertheless, recent interest in microscale and nanoscale radiative heat transfer [1, 2, 3, 4, 6], together with the development of local-probe thermal microscopy [5] have raised new challenges. These topics, and the progress in detecting non-contact friction on sub-attonewton level [7, 8, 9, 10, 11], and the observation of coherent thermal emission from doped silicon and silicon carbide (SiC) gratings [12] have in common the substantial role of the nonradiative (evanescent) thermal field.

It is well known that the radiative heat transfer between two bodies separated by  $d >> \lambda_T = c\hbar/k_B T$  is given by the Stefan-Boltzmann law:

$$S = \frac{\pi^2 k_B^4}{60\hbar^3 c^2} \left( T_1^4 - T_2^4 \right), \tag{1}$$

where  $T_1$  and  $T_2$  are the temperatures of solid 1 and 2, respectively. In this limiting case the heat transfer between two black bodies is determined by the propagating electromagnetic waves radiated by the bodies, and does not depend on the separation d. For  $d < \lambda_T$  the heat transfer increases by many orders of magnitude due to the evanescent electromagnetic waves that decay exponentially into the vacuum; this is often refereed to as photon tunneling. At low temperatures (a few K) it is possible for this form of heat transfer to be dominant even at spacing of a few mm, see table 1.

**Table 1**. Critical distance  $\lambda_T$  as a function of temperature. For surface separation  $d < \lambda_T$  the heat transfer is dominated by the contribution from

the evanescent electromagnetic modes. At distances of a few nanometers, radiative heat flow is almost entirely due to evanescent modes.

$T(\mathbf{K})$	$\lambda_T(\mu \mathrm{m})$
1	2298.8
4.2	545.2
100	22.9
273	8.4
1000	2.3

The problem of the radiative heat transfer between two flat surfaces was considered some years ago by Polder and Van Hove [1], Levin and Rytov [2] and more recently by Pendry [3], and by Volokitin and Persson [4, 6]. In [3, 4, 6] it was shown that the heat flux can be greatly enhanced if the electrical conductivities of the materials are chosen such as to maximize the heat flow due to photon tunneling. At room temperature the heat flow is maximal for materials with conductivities corresponding to semi-metals. In fact, only a thin film ( $\sim 10$ Å) of a high-resistivity material is needed to maximize the heat flux [4]. Another enhancement mechanism of the radiative heat transfer may arise from resonant photon tunneling between localized states on the different surfaces, if the frequency of these modes is sufficiently low to be excited by thermal radiation. Recently, it was predicted enhancement of the heat transfer due to resonant photon tunneling between surface plasmon modes localized on the surfaces of the semiconductors [13, 6] and adsorbate vibrational modes [6].

The problem of radiative heat transfer is closely related to the non-contact friction between nanostructures, including, for example, the frictional drag force between two-dimensional quantum wells [14, 15, 16], and the friction force between an atomic force microscope tip and a substrate [7, 8, 9, 10, 11]

Recently several groups have observed unexpectedly large long-range noncontact friction [7, 8, 9, 10, 11]. The friction force F acting on an atomic force microscope tip was found to be proportional to the velocity  $v, F = \Gamma v$ . At the separation d = 100Å the friction coefficient  $\Gamma \approx 10^{-10} - 10^{-13}$ kg/s. Although the non-contact friction must have an electromagnetic origin, the detailed mechanisms is not fully understood yet.

In a recent Letter, Dorofeyev *et.al.* [7] claim that the non-contact friction observed in [7, 8] is due to Ohmic losses mediated by the fluctuating electromagnetic field. This result is controversial, however, since the van der Waals friction has been shown [17, 18] to be many orders of magnitude smaller than

the friction observed by Dorofeyev *et.al.* However, we have shown that when the surfaces are separated by about 1nm, the van der Waals friction can be greatly enhanced by resonant photon tunneling [19, 20]. Thus, we found that resonant photon tunneling between two semiconductors surfaces of SiC, which can support surface plasmon modes in mid-infrared region, may give rise a 1000-fold (or more) enhancement of the friction, in comparison with the case of good conductors. Furthermore, resonant photon tunneling between two Cu(100) surface covered by 0.1 monolayer of K may result in six orders of magnitude enhancement of friction compared to clean surfaces. At the separation 1nm we obtained a friction comparable in magnitude with the friction observed in the experiment [9].

The origin of the van der Waals friction is very closely connected with ordinary (attractive) van der Waals interaction. The van der Waals interaction between atoms (or molecules) arises from quantum fluctuations in the electric dipole moment of atoms. The short-lived atomic polarity can induce a dipole moment in a neighboring atom or molecule at some distance away. The same is true for extended solids, where thermal and quantum fluctuation of the current density in one body induces a current density in another body. When two bodies are in relative motion, the induced current will lag slightly behind the fluctuating current inducing it, this lag is the origin of the van der Waals friction.

In contrast to the van der Waals interaction, for which a well established theory exist [21], the field of van der Waals friction is still controversial. Thus different authors [22, 23, 24, 25, 26, 27] have derived expression for the van der Waals friction between two flat surfaces and between a small particle and flat surface using different methods, and obtained results, which were not confirmed in subsequent calculations [28, 29, 30, 17, 32].

In [17] we have developed the theory of the van der Waals friction based on a dynamical modification of the well known Lifshitz theory [31] of the van der Waals interaction. In the nonretarded limit, and for zero temperature, this theory agree with the results of Pendry [29]. We have also calculated the van der Waals friction between two flat surfaces in normal relative motion [19, 20], and found a drastic difference in comparison with parallel relative motion. In the limit, when one of the bodies is sufficiently rarefied, our theory gives the friction between flat surface and small particle, which agrees with the results of Tomassone and Widom [33].

The organization of this article is as follows. In Sec.2 we present a short overview of the main principles of the radiative heat transfer, focusing mainly on the adsorbate vibrational mode enhancement of the radiative heat transfer. In Sec.3 we study the van der Waals friction, and its enhancement due to surface polaritons and adsorbates. In the light of our theoretical results, we also discuss non-contact friction experiments. Finally, Sec.4 contains the summary.

## 2 Radiative heat transfer

#### 2.1 Clean surfaces

According to [1, 2, 3, 4] the heat transfer between two semi-infinite bodies, separated by a vacuum gap with the width d, is given by the formula

$$S = \int_0^\infty d\omega \left(\Pi_1 - \Pi_2\right) M \tag{2}$$

where

$$M = \frac{1}{4\pi^2} \int_0^{\omega/c} dq \, q \frac{(1 - |R_{1p}(\omega)|^2)(1 - |R_{2p}(\omega)|^2)}{|1 - e^{2ipd}R_{1p}(\omega)R_{2p}(\omega)|^2} + \frac{1}{\pi^2} \int_{\omega/c}^{\infty} dq \, q e^{-2kd} \times \frac{\mathrm{Im}R_{1p}(\omega)\mathrm{Im}R_{2p}(\omega)}{|1 - e^{-2|p|d}R_{1p}(\omega)R_{2p}(\omega)|^2} + [p \to s], \qquad (3)$$

and where the symbol  $[p \to s]$  stands for the terms which are obtained from the first two terms by replacing the reflection coefficient  $R_p$  for *p*-polarized electromagnetic waves with the reflection coefficient  $R_s$  for *s*- polarized electromagnetic waves, and where  $p = ((\omega/c)^2 - q^2)^{1/2}$ , and k = |p|. The Planck function of solid **1** 

$$\Pi_1(\omega) = \hbar \omega \left( e^{\hbar \omega / k_B T_1} - 1 \right)^{-1}, \tag{4}$$

and similar for  $\Pi_2$ . The contributions to the heat transfer from the propagating  $(q < \omega/c)$  and evanescent  $(q > \omega/c)$  electromagnetic waves are determined by the first and the second terms in Eq.(3), respectively.

From Eq.(3) it is easy to see that the propagating photon modes give the main contribution to the heat transfer for  $q < \lambda_T^{-1}$ , while the evanescent modes for q < 1/d. Thus from phase space arguments it follows that the number of the channels of the heat transfer available for evanescent waves will be by a factor  $(\lambda_T/d)^2$  larger than the number of the channel available for propagating waves. At d = 1nm and T = 300K, this ratio is of the order  $\sim 10^8$ . Let us firstly consider some general consequences of Eq. (3). In the case of the heat transfer through free photons  $(q \leq \omega/c)$ , the transfer is maximal when both the bodies are perfectly black and have zero reflection amplitude  $R = R_r + iR_i = 0$ . The heat flux due to the evanescent waves is a maximal when [3]

$$R_r^2 + R_i^2 = e^{2kd} \tag{5}$$

Substituting this result into (3) gives the maximal contribution from the evanescent waves

$$(S_z)_{max}^{evan} = \frac{k_B^2 T^2 q_c^2}{24\hbar} \tag{6}$$

where  $q_c$  is a cut-off in q, determined by the properties of the material. It is clear that the largest possible  $q_c \sim 1/b$ , where b is an inter-atomic distance. Thus, from Eqs.(6) and (1) we get the ratio of the maximum heat flux connected with evanescent waves to the heat flux due to black body radiation  $(S_z)_{max}/S_{BB} \approx 0.25 \cdot (\lambda_T/b)^2$ . Thus, at room temperature the contribution to the heat flux from evanescent waves may be eight orders of magnitude larger than the contribution from the black body radiation, and the upper boundary for the heat transfer at room temperature:  $(S_z)_{max} \sim 10^{11} \text{Wm}^{-2}$ .

Let us now apply the general theory to a few different materials. For good conductors, using Fresnel formulas for reflection coefficient and assuming  $k_B T/4\pi\hbar\sigma \ll 1$ , and  $\lambda_T (k_B T/4\pi\hbar\sigma)^{3/2} < d < \lambda_T (k_B T/4\pi\hbar\sigma)^{-1/2}$  ( $\sigma$  is the conductivity) the contribution to the heat transfer from *p*-polarized waves for good conductors ( $k_B T/4\pi\hbar\sigma \ll 1$ ) is given by

$$S_p \approx 0.2 \frac{(k_B T)^2}{\hbar \lambda_T d} \left(\frac{k_B T}{4\pi \hbar \sigma}\right)^{1/2},\tag{7}$$

and for the metal with lower conductivity (  $k_B T/4\pi\hbar\sigma \leq 1$ ), for  $d < \lambda_T (k_B T/4\pi\hbar\sigma)^{-1/2}$ we get

$$S_p \approx 0.12 \frac{(k_B T)^2}{\hbar d^2} \left(\frac{k_B T}{4\pi\hbar\sigma}\right)^2 \left(1 + \ln\frac{4\pi\hbar\sigma}{k_B T}\right).$$
(8)

For good conductors the heat flux depends on the separation as  $\sim d^{-1}$ , and increases with decreasing conductivity as  $\sigma^{-1/2}$ . For  $k_B T/4\pi\hbar\sigma \leq 1$ the heat flux decreases with separation as  $d^{-2}$ , and increases with decreasing conductivity as  $\sigma^{-2}$ , while the *s*-wave contribution is distance independent,  $S_s \approx 0.25 k_B T \sigma / \lambda_T^2$ . Fig. 1a shows the heat transfer between two

semi-infinite silver bodies separated by the distance d, at the temperatures  $T_1 = 273$ K and  $T_2 = 0$ K. The s- and p-wave contributions are shown separately. The *p*-wave contribution has been calculated using non-local optics, i.e. including spatial dispersion of the dielectric function (the dashed line shows the result using local optics). It is remarkable how important the s-contribution is even for short distances. Note from Fig.1a that the local optics contribution to  $S_p$  depends nearly linearly on 1/d in the studied distance interval, and that this contribution is much smaller than the s-wave contribution. Both these observations agree with analytical formulas given above. However, for the very high-resistivity materials, the *p*-wave contribution becomes much more important, and a crossover to a  $1/d^2$ -dependence of  $S_p$  is observed at short separations d. This is illustrated in Fig.1b and 1c, which show results for the same parameters as in Fig. 1a, except that the electron mean free path has been reduced from l = 560 Å (the electron mean free path for silver at room temperature) to 20 Å (roughly the mean free path in lead at room temperature) (Fig. 1b) and 3.4 Å (of order the lattice constant, representing the minimal possible mean free path) (Fig. 1c). Note that when l decreases, the *p*-wave contribution to the heat transfer increases while the s-wave contribution decreases. Since the mean free path cannot be much smaller than the lattice constant, the result in Fig. 1c represent the largest possible *p*-wave contribution for normal metals. However, the *p*-wave contribution may be even larger for other materials, e.g., semimetals, with lower carrier concentration than in normal metals. For high resistivity materials, when  $k_B T / 4\pi \hbar \sigma > 1$  the heat flux is proportional to the conductivity

$$S_p \approx 0.2 \frac{k_B T \sigma}{d^2} \tag{9}$$

Figure 2 show the thermal flux as a function of the conductivity of the solids. Again we have assumed that one body is at zero temperature and the other at T = 273K. The surfaces are separated by d = 10 Å. The heat flux for other separations can be obtained using scaling  $\sim 1/d^2$  which holds for highresistivity materials. The heat flux is maximal at  $\sigma = 1316(\Omega \cdot m)^{-1}$ . Finally, we note that thin high-resistivity coatings can drastically increase the heat transfer between two solids. This is illustrated in Fig.3, which shows the heat flux for the case when thin films ( $\sim 10$  Å) of high resistivity material,  $\rho = 0.14 \ \Omega \cdot cm$ , are deposited on silver. (a) and (b) shows the *p*- and *s*contributions, respectively. Also shown are the heat flux when the two bodies are made from silver, and from the high resistivity material. It is interesting to note that while the *p*-wave contribution to the heat flux for the coated surfaces is strongly influenced by the coating, the *s*-contribution is nearly unaffected.

Another case where the heat transfer can be large is when resonant photon tunneling occurs between surface states localized on the different surfaces. The resonant condition corresponds to the case when the denominators in Eq.(3) are small. For two identical surfaces and  $R_i \ll 1 \leq R_r$ , where  $R_i$ and  $R_r$  are the imaginary and real parts of the reflection coefficient, this corresponds to the resonant condition

$$R_r \exp(-qd) = \pm 1 \tag{10}$$

This condition can be fulfilled in spite of the factor  $\exp(-2qd) < 1$  because for evanescent electromagnetic waves there is no restriction on the magnitude of real part or the modulus of R. This opens up the possibility of resonant denominators for  $R_r^2 \gg 1$ . Close to the resonance we can use the approximation

$$R = \frac{\omega_a}{\omega - \omega_0 - i\eta},\tag{11}$$

where  $\omega_a$  is a constant. Then from the resonant condition  $(R_r = \pm e^{qd})$  we get the positions of the resonance

$$\omega_{\pm} = \omega_0 \pm \omega_a e^{-qd}.$$

For the resonance condition to be valid the separation  $\Delta \omega = |\omega_+ - \omega_-|$ between two resonances must be greater than the width  $\eta$  of the resonance. From this condition we get that the two poles approximation is valid for  $q \leq q_c \approx \ln(2\omega_a/\eta)/d$ .

For  $\omega_0 > \omega_a$  and  $q_c d > 1$ , we get

$$S_{\pm} = \frac{\eta q_c^2}{4\pi} \left[ \Pi_1(\omega_0) - \Pi_2(\omega_0) \right].$$
 (12)

Note, that the explicit d dependence has dropped out of Eq. (12). However, S may still be d- dependent, through the d- dependence of  $q_c$ . For small distances one can expect that  $q_c$  is determined by the dielectric properties of the material, and thus does not depend on d. In this case the heat transfer will also be distance independent. Resonant photon tunneling enhancement of the heat transfer is possible for two semiconductor surfaces which can support low-frequency surface plasmon modes in the mid-infrared frequency region. The reflection factor  $R_p$  for clean semiconductor surface at  $d < \lambda_T |\epsilon|^{-1/2}$  is given by Fresnel's formula

$$R_p = \frac{\epsilon - 1}{\epsilon + 1},\tag{13}$$

where  $\epsilon$  is the bulk dielectric function. As an example, consider two clean surfaces of silicon carbide (SiC). The optical properties of this material can be described using an oscillator model [34]

$$\epsilon(\omega) = \epsilon_{\infty} \left( 1 + \frac{\omega_L^2 - \omega_T^2}{\omega_T^2 - \omega^2 - i\Gamma\omega} \right)$$
(14)

with  $\epsilon_{\infty} = 6.7$ ,  $\omega_L = 1.83 \cdot 10^{14} s^{-1}$ ,  $\omega_T = 1.49 \cdot 10^{14} s^{-1}$ , and  $\Gamma = 8.9 \cdot 10^{11} s^{-1}$ . The frequency of surface plasmons is determined by condition  $\epsilon_r(\omega_p) = -1$ and from (14) we get  $\omega_p = 1.78 \cdot 10^{14} s^{-1}$ . The resonance parameters

$$\omega_a = \frac{\omega_L^2 - \omega_T^2}{\epsilon_{\infty}\omega_L} = 8.2 \cdot 10^{12} \text{s}^{-1}, \ \eta = \Gamma/2, \ q_c = 3.6/d, \text{ and } \omega_0 \approx \omega_p$$

Using these parameters in Eq.(12) and assuming that one surface is at temperature T = 300 K and the other at 0 K we get the heat flux S(d) between two clean surfaces of silicon carbide (SiC):

$$S_p \approx 8.4 \cdot 10^9 \frac{1}{d^2} \text{W} \cdot \text{m}^{-2}$$
 (15)

where the distance d is in Angstrøm. Note that the heat flux between the two semiconductor surfaces is several order of magnitude larger than between two clean good conductor surfaces (see Fig.1).

# 2.1.1 Adsorbate vibrational mode enhancement of the radiative heat transfer

Another resonant photon tunneling enhancement of the heat transfer is possible between adsorbate vibrational modes localized on different surfaces. Let us consider two particles or adsorbates with the dipole polarizabilities  $\alpha_1(\omega)$ and  $\alpha_2(\omega)$  and with the fluctuating dipole moments  $p_1^f$  and  $p_2^f$  normal to the surfaces. Accordingly to the fluctuation-dissipation theorem [35], the power spectral density for the fluctuating dipole moment is given by

$$\langle p_i^f p_j^f \rangle_\omega = \frac{\hbar}{\pi} \left( \frac{1}{2} + n_i(\omega) \right) \operatorname{Im} \alpha_i(\omega) \delta_{ij}$$
 (16)

where the Bose-Einstein factor

$$n_i(\omega) = \frac{1}{e^{\hbar\omega/k_B T_i} - 1}.$$
(17)

Assume that the particles are situated opposite to each other on two different surfaces, at the temperatures  $T_1$  and  $T_2$ , respectively, and separated by the distance d. The fluctuating electric field of a particle 1 does work on a particle 2. The rate of working is determined by

$$P_{12} = 2 \int_0^\infty d\omega \,\omega \mathrm{Im}\alpha_2(\omega) \langle E_{12} E_{12} \rangle_\omega \tag{18}$$

where  $E_{12}$  is the electric field created by a particle **1** at the position of a particle **2**:

$$E_{12} = \frac{8p_1^f/d^3}{1 - \alpha_1 \alpha_2 (8/d^3)^2}$$
(19)

From Eqs. (16-18) we get  $P_{12}$ , and the rate of cooling of a particle **2** can be obtained using the same formula by reciprocity. Thus the total heat exchange power between the particles is given by

$$P = P_{12} - P_{21} = \frac{2\hbar}{\pi} \int_0^\infty d\omega \,\omega \frac{\mathrm{Im}\alpha_1 \mathrm{Im}\alpha_2 (8/d^3)^2}{\left|1 - (8/d^3)^2 \alpha_1 \alpha_2\right|^2} (n_1(\omega) - n_2(\omega)) \tag{20}$$

Let us firstly consider some general consequences of Eq. (20). There are no constrain on the particle polarizability  $\alpha(\omega) = \alpha' + i\alpha''$  other than that  $\alpha''$  is positive, and  $\alpha'$  and  $\alpha''$  are connected by the Kramers-Kronig relation. Therefore, assuming identical surfaces, we are free to maximize the photon-tunneling transmission coefficient

$$t = \frac{(8\alpha''/d^3)^2}{\left|1 - (8\alpha/d^3)^2\right|^2} \tag{21}$$

This function has a maximum when

$$\alpha'^2 + \alpha''^2 = (d^3/8)^2 \tag{22}$$

so that t = 1/4. Substituting this result in (20) gives the upper bound for the heat transfer power between the two particles or adsorbates

$$P_{max} = \frac{\pi k_B^2}{3\hbar} (T_1^2 - T_2^2) \tag{23}$$

For adsorbed molecules at the concentration  $n_a = 10^{19} \text{m}^{-2}$ , when one surface is at zero temperatures and the other is at the room temperature, the maximal heat flux due to the adsorbates  $S_{max} = n_a P_{max} = 10^{12} \text{Wm}^{-2}$ , which is nearly 10 order of magnitude larger than the heat flux due to the black body radiation,  $S_{BB} = \sigma_B T = 4 \cdot 10^2 \text{Wm}^{-2}$ , where  $\sigma_B$  is the Boltzmann constant. The conditions for resonant photon tunneling are determined by equation

$$\alpha'(\omega_{\pm}) = \pm d^3/8 \tag{24}$$

Close to resonance we can use the approximation

$$\alpha \approx \frac{c}{\omega - \omega_0 - i\eta},\tag{25}$$

where  $c = e^{*2}/2M\omega_0$ , and where  $e^*$  and M are the dynamical charge and mass of the adsorbate, respectively. Then from the resonant condition (24) we get

$$\omega_{\pm} = \omega_0 \pm 8c/d^3.$$

The separation between the resonances,  $\Delta \omega = |\omega_+ - \omega_-|$  must be greater than the width  $\eta$  of the resonance, so that  $8c/d^3 > \eta$ .

For  $\eta \ll 8c/d^3$ , from Eq. (20) we get

$$P = \frac{\hbar\eta}{2} [\omega_{+}(n_{1}(\omega_{+}) - n_{2}(\omega_{+})) + (+ \to -)], \qquad (26)$$

Using Eq. (26) we can estimate the heat flux between identical surfaces covered by adsorbates with concentration  $n_a$ :  $S \approx n_a P$ . Interestingly, the explicit *d* dependence has dropped out of Eq. (26). However, *P* may still be *d*- dependent, through the *d*- dependence of  $\omega_{\pm}$ . For  $\hbar \omega_{\pm} \leq k_B T$  the heat transfer will be only weakly distance dependent. For  $8c/d^3 < \eta$  we can neglect multiple scattering of the photons between the particles, so that the denominator in the integrand in Eq. (20) can be approximated with unity. For d >> b, where *b* is the interparticle spacing, the heat flux between two surfaces covered by adsorbates with concentration  $n_{a1}$  and  $n_{a2}$  can be obtained after integration of the heat flux between two separated particles. We get

$$S = \frac{24\hbar n_{a1}n_{a2}}{d^4} \int_0^\infty d\omega \,\omega \mathrm{Im}\alpha_1 \mathrm{Im}\alpha_2 [n_1(\omega) - n_2(\omega)] \tag{27}$$

Assuming that  $\alpha$  can be approximated by Eq. (25), for  $\omega_0 \ll \eta$  Eq. (27) gives the heat flux between two identical surfaces:

$$S = \frac{12\pi\hbar\omega_0 c^2 n_a^2}{d^4\eta} [n_1(\omega_0) - n_2(\omega_0)]$$
(28)

For the K/Cu(001) system  $\omega_0 = 1.9 \cdot 10^{13} \text{s}^{-1}$ , and at low coverage  $e^* = 0.88e$  [36], which gives  $c = e^{*2}/2M\omega_0 = 7 \cdot 10^{-17} \text{ m}^3 \text{s}^{-1}$ . For  $\eta = 10^{12} \text{s}^{-1}$ , when one surface has T = 300K and the other T = 0K, for d > b and  $8a/d^3 < \eta$  we get

$$S \approx 5.6 \cdot 10^{-24} \frac{n_a^2}{d^4} \,\mathrm{W} \cdot \,\mathrm{m}^{-2}$$
 (29)

where the d is in Ångstrøm.

We note that Eq.(28) can be obtained directly from the heat flux between two semi-infinite solids determined by Eq.(3), since in the limit d > b we can use a macroscopic approach, where all the information about the optical properties of the surface is included in reflection coefficient [6]. The reflection coefficient  $R_p$ , which take into account the contribution from an adsorbate layer is given by [41]:

$$R_p = \frac{1 - s/q\epsilon + 4\pi n_a [s\alpha_{\parallel}/\epsilon + q\alpha_{\perp}] - qa(1 - 4\pi n_a q\alpha_{\parallel})}{1 + s/q\epsilon + 4\pi n_a [s\alpha_{\parallel}/\epsilon - q\alpha_{\perp}] + qa(1 + 4\pi n_a q\alpha_{\parallel})},$$
(30)

where  $s = \sqrt{q^2 - (\omega/c)^2 \epsilon}$ , and  $\alpha_{\parallel}$  and  $\alpha_{\perp}$  are the polarizabilities of adsorbates in a direction parallel and normal to the surface, respectively.  $\epsilon = 1 + 4\pi i \sigma / \omega$  is the bulk dielectric function, where  $\sigma$  is a conductivity, and  $n_a$  is the concentration of adsorbates. Eq.(30) takes into account that the centers of the adsorbates are located at distance a away from image plane of the metal. Although this gives corrections of the order  $qa \ll 1$  to the reflection amplitude, for parallel adsorbate vibrations on the good conductors (when  $\epsilon \gg 1$ ), in some cases they give the most important contribution to the energy dissipation. As illustration of this macroscoscopic approach, in Fig.(4) we show the *p*-wave contribution to the heat flux for the two Cu(100) surfaces covered by a low concentration of potassium atoms ( $n_a = 10^{18} \text{m}^{-2}$ ) and the two clean Cu(100) surfaces. At separation d = 1nm the heat flux between two surfaces covered by adsorbates is enhanced by five and three orders of magnitude in comparison with the *p*- and *s*- wave contributions to the heat flux between clean surfaces, respectively, and by seven orders of magnitude in comparison with the blackbody radiation.

For d < b the macroscopic approach is not valid any more and we must sum the heat flux between each pair of the adatoms. For  $\eta = 10^{12} \text{s}^{-1}$  and  $d < 10\text{\AA}$ , when one surface has T = 300K and the other T = 0K, from Eq.(26) we get the distance independent  $P \approx 10^{-9}\text{W}$ . In this case, for  $n_a =$  $10^{18}\text{m}^{-3}$  the heat flux  $S \approx Pn_a \approx 10^9 \text{Wm}^{-2}$ . Under the same conditions the *s*-wave contribution to the heat flux between two clean surfaces  $S_{clean} \approx$  $10^6 \text{Wm}^{-2}$ . Thus the photon tunneling between the adsorbate vibrational states can strongly enhance the radiative heat transfer between the surfaces. However this enhancement of the heat flux disappears if only one of the surfaces is covered by adsorbates.

It is interesting to note that in the strong coupling case  $(8c/d^3 \gg \eta)$  the heat flux between two molecules does not depend on the dynamical dipole moments of the molecules (see Eq.(26). However, in the opposite case of the weak coupling  $(8c/d^3 \ll \eta)$  the heat flux is proportional to the product of the squares of the dynamical dipole moments (see Eq.(28)).

## 3 Van der Waals friction

#### **3.1** Clean surfaces

The frictional stress  $\sigma_{\perp(\parallel)}$  which act on the surfaces of two bodies in normal (parallel) relative motion can, to linear order in sliding velocity v, be written in the form:  $\sigma_{\perp(\parallel)} = \gamma_{\perp(\parallel)}v$ . For bodies in parallel relative motion at separation  $d \ll \lambda_T$  the friction coefficient  $\gamma_{\parallel}$  is given by [17]

$$\gamma_{\parallel} = \frac{\hbar}{2\pi^2} \int_0^\infty d\omega \left( -\frac{\partial n}{\partial \omega} \right) \int_{\omega/c}^\infty dq \, q^3 e^{-2kd}$$
$$\times \operatorname{Im} R_{1p} \operatorname{Im} R_{2p} \frac{1}{\left| 1 - e^{-2kd} R_{1p} R_{2p} \right|^2} + [p \to s]. \tag{31}$$

When the two bodies move toward or away from each other the friction

coefficient is given by [19, 20]

$$\gamma_{\perp} = \frac{\hbar}{\pi^2} \int_0^\infty d\omega \left( -\frac{\partial n}{\partial \omega} \right) \int_{\omega/c}^\infty dq \, q k^2 e^{-2kd} \\ \times [(\operatorname{Im} R_{1p} + e^{-2kd} | R_{1p} |^2 \operatorname{Im} R_{2p}) (\operatorname{Im} R_{2p} + e^{-2kd} | R_{2p} |^2 \operatorname{Im} R_{1p}) \\ + e^{-2kd} (\operatorname{Im} (R_{1p} R_{2p}))^2] \frac{1}{|1 - e^{-2kd} R_{1p} R_{2p}|^4} + [p \to s],$$
(32)

where the Bose-Einstein factor

$$n(\omega) = \frac{1}{e^{\hbar\omega/k_BT} - 1}.$$

At resonance the integrand in Eqs. (32) has a large factor  $\sim 1/R_i^2$ , in sharp contrast to the case of parallel relative motion (see Eq.(31)), where there is no such enhancement factor. Thus, at resonance if  $R_i^2 << 1$  the friction for normal relative motion will be much larger than the friction for parallel relative motion. In contrast to the heat transfer, the van der Waals friction is very sensitive to presence of low frequency excitations which absorb plenty momentum without absorbing much energy. Thus the van der Waals friction is very sensitive to the type of the material.

Assuming that the medium **2** is sufficiently rarefied and consist of particles with the radius  $r \ll d$ , with the polarizability  $\alpha(\omega)$  given by Eq.(31), it is easy to calculate friction coefficient between a small particle and a flat surface:

$$\Gamma_{\parallel} = \frac{\hbar}{\pi} \int_{0}^{\infty} d\omega \omega \left( -\frac{\partial n}{\partial \omega} \right) \int_{0}^{\infty} dq q^{2} e^{-2qd} \operatorname{Im} \alpha_{2} \\ \times \left\{ 2 \operatorname{Im} R_{1p} \left[ 2 + \left( \frac{\omega}{cq} \right)^{2} \right] + \left( \frac{\omega}{cq} \right)^{2} \operatorname{Im} R_{1s}(\omega) \right\}$$
(33)

and  $\Gamma_{\perp} = 2\Gamma_{\parallel}$ . In the nonretarded limit  $(c \to \infty)$  this formula agrees with the result obtained in [33].

For good metals  $(k_B T/4\pi\hbar\sigma >> 1)$  using (32) for  $\lambda_T (k_B T/4\pi\hbar\sigma)^{3/2} < d < \lambda_T (4\pi\hbar\sigma/(k_B T)^{1/2})$  ( $\lambda_T = c\hbar/(k_B T)$ ), we get

$$\gamma_{\perp p} \approx 0.13 \frac{\hbar}{d^3 \lambda_T} \left(\frac{k_B T}{4\pi \hbar \sigma}\right)^{1/2},$$
(34)

and for  $d < \lambda_T (k_B T / 4\pi \hbar \sigma)^{3/2}$  we get

$$\gamma_{\perp p} \approx \frac{\hbar}{d^4} \left(\frac{k_B T}{4\pi\hbar\sigma}\right)^2 \left(1 + \ln\frac{\hbar\sigma}{2k_B T}\right).$$
 (35)

The last contribution will dominate for metal with not too high conductivity  $(k_B T/4\pi\hbar\sigma \simeq 1)$ .

For comparison, the *p*-wave contribution for parallel relative motion for  $d < \lambda_c$ ,  $(\lambda_c = c/(4\pi\sigma k_B T)^{1/2})$  is given by [17]

$$\gamma_{\parallel p}^{evan} \approx 0.3 \frac{\hbar}{d^4} \left(\frac{k_B T}{4\pi\hbar\sigma}\right)^2 \tag{36}$$

It is interesting to note that, in contrast to parallel relative motion, for normal relative motion of good conductors, for practically all d > 0 the main contribution to friction comes from retardation effects, since Eq. (34), in contrast to Eq. (36), contains the light velocity.

From Eq. (32) we get the s-wave contribution to friction for  $d < \lambda_c$ 

$$\gamma_{\perp s}^{evan} \approx 10^{-2} \frac{\hbar}{\lambda_c^4} (3 - 5 \ln(2d/\lambda_c)) \tag{37}$$

For parallel relative motion the s-wave contribution is two times smaller:  $\gamma_{\perp s}^{evan} = 2\gamma_{\parallel s}^{evan}$ .

Figures 5 and 6 show the calculated contribution to the friction coefficient  $\gamma$  from the evanescent electromagnetic waves for two semi-infinite solids, with parameters chosen to correspond to copper  $(\tau^{-1} = 2.5 \cdot 10^{13} s^{-1})$  $\omega_p = 1.6 \cdot 10^{16} s^{-1}$ ) at T = 273 K, for parallel (Fig.5) and normal (Fig.6) relative motion. Results are shown separately for both the s- and p- wave contribution. The dashed line shows the result when the local (long-wavelength) dielectric function  $\epsilon(\omega)$  is used, and the full line show the result obtained within the non-local optic dielectric formalism, which was proposed some years ago for the investigation of the optical properties of metals in anomalous skin effect frequency region [37]. Fig.5 shows that, for sufficiently small separations (d < 1000 Å), for parallel relative motion the non-local optic effects become important for the p- wave contribution. However, for the swave contribution, for both parallel and normal relative motion, the nonlocal optic effects are negligibly small for practically all the separations. For normal relative motion, for the *p*-wave contribution the non-local optic effects are less important, than for the parallel relative motion.

For high-resistivity metals  $(k_B T/4\pi\hbar\sigma > 1)$  for  $d < \lambda_c$  we get

$$\gamma_{\perp} \approx 0.48 \frac{\hbar}{d^4} \frac{k_B T}{4\pi\hbar\sigma} \tag{38}$$

and  $\gamma_{\parallel} \approx 0.1 \gamma_{perp}$ . Thus, in contrast to the heat flux, the van der Waals friction diverges in the limit  $\sigma \to 0$ . Of course, in reality the friction must vanish in this limit since the conductivity is proportional to concentration of free electrons, and the friction must vanish as the carrier concentration vanishes. The origin of the discrepancy lies in the breakdown of the macroscopic theory which was used in the calculation of friction at low electron concentration. The macroscopic approach for the electromagnetic properties of material is valid only when the length scale of the spatial variation of the electromagnetic field is much larger than the average distance between the electrons. For evanescent waves this length scale is determined by the separation d between the bodies. Thus, the macroscopic approach is valid if  $d >> n^{-1/3}$ , where n is the concentration of electrons. This fact was overlooked in Ref.[40]. From this requirement we can estimate the maximum friction which can be obtained for high resistivity metals. The minimum conductivity can be estimated as

$$\sigma_{\min} \sim \frac{e^2 \tau}{d^3 m}$$

and the maximum of friction

$$\gamma_{\rm max} \sim \frac{\hbar}{d^4} \frac{k_B T}{4\pi \hbar \sigma_{\rm min}} \sim \frac{m k_B T}{4\pi e^2 \tau d}$$

To estimate the friction coefficient  $\Gamma$  for an atomic force microscope tip with radius of curvature r >> d we can use an approximate formula [38, 39]

$$\Gamma = 2\pi \int_0^\infty d\rho \rho \gamma(z(\rho)) \tag{39}$$

where it is assumed that the tip has cylinder symmetry. Here  $z(\rho)$  denotes the tip - surface distance as a function of the distance  $\rho$  from the tip symmetry axis, and the friction coefficient  $\gamma(z(\rho))$  is determined by the expressions for flat surfaces. We assume that the tip has a paraboloid shape given [in cylindrical coordinates  $(z, \rho)$ ] by the formula:  $z = d + \rho^2/2r$ . If

$$\gamma(\rho) = \frac{C}{\left(d + \frac{\rho^2}{2r}\right)^n} \tag{40}$$

we get

$$\Gamma = \frac{2\pi r}{n-1} \frac{C}{d^{n-1}} = \frac{2\pi r d}{n-1} \gamma(d) = A_{eff} \gamma(d)$$

where  $A_{eff}$  is the effective surface area. For high-resistivity metals n = 4, and the maximum friction coefficient for spherical tip:

$$\Gamma_{\max}^s \sim \gamma_{max} dr \sim \frac{mk_B Tr}{4\pi e^2 \tau}$$

Using this formula for  $\tau \sim 10^{-15}s$ ,  $r \sim 1\mu m$  and T = 300K we get  $\Gamma_{\text{max}} \sim 10^{-15} kg/s$ . This friction is two order of magnitude smaller than was observed in a recent experiment [9] at d = 10 nm. In the case of the cylindrical tip with the width w:

$$\Gamma_{\rm max}^c \sim \gamma_{max} \sqrt{dr} w \sim \frac{mk_B T w R^{0.5}}{4\pi e^2 \tau d^{0.5}}$$

For  $w = 7\mu m$  and d = 10nm the friction is of the same order as it was observed in experiment. Thus, van der Waals friction between high resistivity material can be measured with the present state-of-art equipment.

As in the case of the radiative heat transfer, the van der Waals friction can be greatly enhanced when resonant photon tunneling between localized surface states, e.g. surface plasmon polaritons and adsorbate vibration modes, occurs. Using the same approximation as when deriving Eq.(12) for normal relative motion we get

$$\gamma_{\perp} = \frac{3}{128} \frac{\hbar^2 \omega_a^2}{d^4 k_B T \eta} \frac{1}{\sinh^2(\hbar \omega_0 / 2k_B T)}.$$
(41)

Similar, for parallel relative motion

$$\gamma_{\parallel} = \frac{\hbar^2 \eta q_c^4}{128\pi k_B T} \frac{1}{\sinh^2(\hbar\omega_0/2k_B T)}$$
(42)

where  $q_c = \min(b, \ln(2\omega_a/\eta)/d)$ , and where b is of the order of an interatomic distance. Thus if  $\ln(2\omega_a/\eta)/d > b$ , Eq. (42) is independent of the distance. For small distances one can expect that  $q_c$  is determined by the dielectric properties of the material, and does not depend on d. In this case the friction will be also distance independent.

Resonant photon tunneling enhancement of the van der Waals friction is possible for two semiconductor surfaces which can support low-frequency surface plasmon modes. As an example we consider two clean surfaces of silicon carbide (SiC). The optical properties of this material were described above. Using the same parameters as before and at T = 300K we get  $\gamma_{\parallel} \approx (10^3/d^4)$ kg· s<sup>-1</sup>m<sup>-2</sup>, where the distance d is in Ångstrøm, and  $\gamma_{\perp} \approx 3\gamma_{\parallel}$ . Note that the friction between the two semiconductors is about three order of magnitude larger than between two clean good metallic conductors (see Fig.(5,6)).

# 3.2 Adsorbate vibrational mode enhancement of the van der Waals friction

Another enhancement mechanism of van der Waals friction is connected with resonant photon tunneling between adsorbate vibrational modes localized on different surfaces. In [19, 20] we have shown that resonant photon tunneling between two surfaces covered by a low coverage of potassium atoms at d = 1nm gives rise to enhancement in friction by six orders of the magnitude in the comparison with friction between clean surfaces. The adsorbate induced enhancement of van der Waals friction is even larger for the case of Cs adsorption on Cu(100). In this case even at small coverage ( $\theta \approx 0.08$ ) in adsorbed layer there is acoustic branch for vibrations parallel to the surface [36]. In this case at small frequencies the reflection coefficient is given by [41]

$$R_p = 1 - \frac{2qa\omega_q^2}{\omega^2 - \omega_q^2 + i\omega\eta} \tag{43}$$

where  $\omega_q^2 = 4\pi n_a e^{*2} a q^2/M$ ,  $\eta$  is the damping constant for the adsorbate vibrations parallel to the surface, a is the separation between the adsorbate center and image plane. Using Eq.(43) in Eq.(31) for

$$\frac{a}{\eta d} \sqrt{\frac{4\pi n_a e^{*2}a}{M d^2}} \ll 1$$

$$\gamma_{\parallel} \approx 0.62 \frac{k_B T a^2}{\eta d^6} \tag{44}$$

we get

It is interesting to note that the dependence on  $n_a$ ,  $e^*$ , and M is dropped out from Eq.(44). However, Eq.(43) is only valid when there are acoustic vibrations in the adsorbed layer. For Cs adsorbed on Cu(100) surface the acoustic vibrations exist only for  $\theta \ge 0.1$  [36]. The friction coefficient for the atomic force microscope can be estimated using approximate Eq.(39). Using Eq.(44) for a cylindrical tip we get

$$\Gamma_{\parallel}^c \approx 0.68 \frac{k_B T a^2 r^{0.5} w}{\eta d^{5.5}} \tag{45}$$

where r is the radius of the curvature of the tip and w is its width. In the case of Cs adsorbed on Cu(100) surface the damping constant  $\eta \approx 3 \cdot 10^9 \text{s}^{-1}$  and a = 2.94 Å [41]. Than for  $r = 1 \mu \text{m}$ ,  $w = 7 \mu \text{m}$ , T = 293 K at d = 10 nm we get  $\Gamma_{\parallel} = 0.5 \cdot 10^{-13} \text{kg/s}$ , that is only three times smaller than the friction observed in [9] at the same distance. However van der Waals friction is characterized by much stronger distance dependence (~  $1/d^{5.5}$ ) than in experiment (~  $1/d^n$ , where  $n = 1.3 \pm 0.2$ ). Thus at smaller distances the van der Waals friction will be much larger than friction observed in [9] and can be measured experimentally. Fig.7 shows the friction coefficient between the copper tip and the copper substrate as a function of the separation d, when the surfaces of the tip and the substrate are covered by low concentration of the Cs atoms and for the clean surfaces. In comparison, the friction between two clean surfaces at the separation d = 1 nm is eleven orders of the magnitude smaller. However, the friction between clean surfaces shown in Fig.(7) was calculated in local optic approximation. For parallel relative motion the nonlocal optic effects are very important (see Fig.5) and when these non-local optic effects are taken into account the friction between adsorbate covered surfaces at d = 1nm will be by seven orders of magnitude larger than the friction between clean surfaces in parallel relative motion.

### 4 Summary

We have studied how the radiative heat transfer and van der Waals friction between two bodies depends on the dielectric properties of the media. We have found that, at short distances between the bodies, the thermal flux can be significantly enhanced in comparison with the black body radiation, in particular when the material involved can support low-frequency adsorbate vibrational modes, or surface plasmon modes, or the conductivity of the metals is chosen to optimize the heat transfer. This fact can be used in the scanning probe microscopy for local heating and modification of surfaces. We have shown that the van der Waals friction can be enhanced by several orders of magnitude in the case of resonant photon tunneling between lowfrequency surface plasmon modes and adsorbate vibrational modes. In the case of friction between two Cu(100) surfaces covered by a low concentration of cesium atoms at d = 10nm we have found the friction to be of the same order of the magnitude as it was observed in experiment [9]. However, the van der Waals friction is characterized by stronger distance dependence than the friction observed in experiment. Thus at small distances the van der Waals friction can be much larger than the friction observed in [9] and can be measured experimentally. This effect can be important technologically for ultrasensitive force registration and from basic point of view. The friction observed in [9] can be explained by *electrostatic* friction [41] when the electromagnetic field in the vacuum gap is mediated by bias voltage or by inhomogeneities of the surfaces.

#### Acknowledgment

A.I.V acknowledges financial support from DFG and Russian Foundation for Basic Research (Grant N 04-02-17606) B.N.J.P. acknowledges support from the European Union Smart Quasicrystals project.

#### FIGURE CAPTIONS

Fig. 1 (a) The heat transfer flux between two semi-infinite silver bodies as a function of the separation d, one at temperature  $T_1 = 273$  K and another at  $T_2 = 0$  K. (b) The same as (a) except that we have reduced the Drude electron relaxation time  $\tau$  for solid 1 from a value corresponding to a mean free path  $v_F \tau = l = 560$  Å to 20 Å. (c) The same as (a) except that we have reduced l to 3.4 Å. For silver (Fig.1a) at T = 273 K the conductivity  $\sigma = 5.6 \cdot 10^{17} \text{s}^{-1}$  and  $k_B T / 4\pi \hbar \sigma = 4.6 \cdot 10^{-6}$  and for Fig.1b and Fig.2c these quantities can be obtained using scaling  $\sigma \sim l^{-1}$ . (The base of the logarithm is 10)

Fig. 2 The thermal flux as a function of the conductivity of the solids. The solid surfaces are separated by d = 10 Å. The heat flux for other separations can be obtained using scaling  $\sim 1/d^2$  which holds for high-resistivity materials. (The base of the logarithm is 10)

Fig. 3. The heat flux between two semi-infinite silver bodies coated with 10 Å high resistivity ( $\rho = 0.14 \ \Omega \text{cm}$ ) material. Also shown is the heat flux between two silver bodies, and two high-resistivity bodies. One body is at zero temperature and the other at T = 273K. (a) and (b) shows the p and s-contributions, respectively. (The base of the logarithm is 10)

Fig. 4. The heat flux between two surfaces covered by adsorbates and between two clean surface, as a function of the separation d. One body is at zero temperature and the other at T = 273 K. For parameters corresponding to K/Cu(001) and Cu(001) [36] ( $\omega_{\perp} = 1.9 \cdot 10^{13} s^{-1}, \omega_{\parallel} = 4.5 \cdot 10^{12} s^{-1}, \eta_{\parallel} = 2.8 \cdot 10^{10} s^{-1}, \eta_{\perp} = 1.6 \cdot 10^{12} s^{-1}, e^* = 0.88e$ ) (The base of the logarithm is 10)

Fig. 5. The friction coefficient for two flat surfaces in parallel relative motion as a function of separation d at T = 273 K with parameter chosen to correspond to copper ( $\tau^{-1} = 2.5 \cdot 10^{13} s^{-1}$ ,  $\omega_p = 1.6 \cdot 10^{16} s^{-1}$ ). The contributions from the s- and p-polarized electromagnetic field are shown separately. The full curves represent the results obtained within the nonlocal optic dielectric formalism, and the dashed curves represent the result obtained within local optic approximation. (The base of the logarithm is 10)

Fig. 6. The friction coefficient for two flat surfaces in normal relative motion as a function of separation d at T = 273 K with parameter chosen to correspond to copper ( $\tau^{-1} = 2.5 \cdot 10^{13} s^{-1}$ ,  $\omega_p = 1.6 \cdot 10^{16} s^{-1}$ ). The contributions from the s- and p-polarized electromagnetic field are shown separately. The full curves represent the results obtained within the nonlocal optic dielectric formalism, and the dashed curves represent the result obtained within local optic approximation. (The base of the logarithm is 10)

Fig. 7. The friction coefficient between the copper tip and copper substrate which surfaces are covered by low concentration of cesium atoms, as a function of the separation d. The cylindrical tip is characterized by radius of curvature  $r = 1\mu$ m and width  $w = 7\mu$ m. For other parameters corresponding to Cs adsorbed on Cu(100) surface at coverage  $\theta \approx 0.1$  and for Cu(100) [36, 41]:  $e^* = 0.28e$ ,  $\eta = 3 \cdot 10^9 \text{s}^{-1}$ ,  $a = 2.94\text{\AA}$ , T = 293 K. (The base of the logarithm is 10)

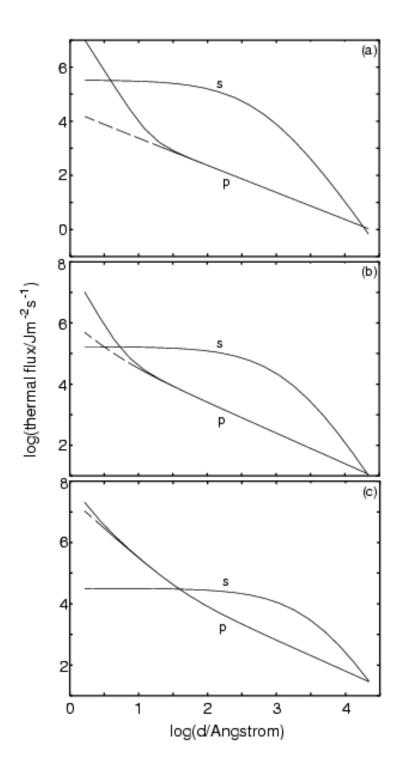
## References

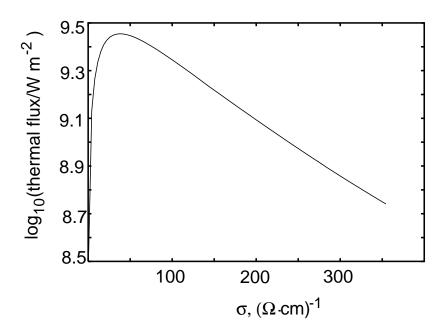
- [1] D.Polder and M.Van Hove, Phys. Rev. B 4, 3303, (1971).
- M.L.Levin, V.G.Polevoy, and S.M.Rytov, Zh.Exsp.Teor.Fiz. 79, 2087 (1980) [Sov.Phys.JETP 52, 1054 (1980)].
- [3] J.B.Pendry, J.Phys.:Condens.Matter **11**, 6621 (1999).
- [4] A.I.Volokitin and B.N.J.Persson, Phys. Rev. B 63, 205404 (2001); Phys. Low-Dim. Struct. 5/6, 151 (2001)

- [5] A.Majumdar, Ann.Rev:Mater.Sci. 29, 505 (1999).
- [6] A.I.Volokitin and B.N.J.Persson, Phys. Rev. B 69, 045417 (2004); JETP Lett. 78, 457(2003)
- [7] I.Dorofeyev, H.Fuchs, G.Wenning, and B.Gostmann, Phys. Rev. Lett. 83, 2402 (1999).
- [8] B.Gostmann and H.Fuchs, Phys. Rev. Lett. 86, 2597 (2001).
- [9] B.C.Stipe, H.J.Mamin, T.D.Stowe, T.W.Kenny, and D.Rugar, Phys. Rev. Lett. 87, 096801 (2001).
- [10] H.J.Mamin and D.Rugar, Appl.Phys. Lett. **79**, 3358 (2001)
- [11] P.M.Hoffmann, S.Jeffery, J.B.Pethica, H.Ozgür Ozer and A.Oral, Phys. Rev. Lett. 87, 265502 (2001).
- [12] J.J.Greffet, R.Carminati, K.Joulain, J.P.Mulet, S.Mainguy, and Y.Chen, Nature, 416, 61(2002)
- [13] J.P.Mulet, K.Joulin, R.Carminati, and J.J.Greffet, Appl. Phys.Lett. 78, 2931 (2001)
- [14] T.J. Gramila, J.P. Eisenstein, A.H. Macdonald, L.N. Pfeiffer, and K.W. West, Phys. Rev. Lett. 66, 1216 (1991); Surf. Sci. 263, 446 (1992).
- [15] T.J. Gramila, J.P. Eisenstein, A.H. Macdonald, L.N. Pfeiffer, and K.W. West, Phys. Rev. B 47, 12 957 (1993); Physica B 197, 442 (1994).
- [16] U. Sivan, P.M. Solomon, and H.Shrikman, Phys. Rev. Lett. 68, 1196 (1992).
- [17] A. I. Volokitin and B. N. J. Persson, J.Phys.: Condens. Matter 13, 859 (2001)
- [18] A. I. Volokitin and B. N. J. Persson, Phys. Rev. Lett. 84, 3504 (2000).
- [19] A. I. Volokitin and B. N. J. Persson, Phys. Rev. Lett. **91**, 106101 (2003).
- [20] A. I. Volokitin and B. N. J. Persson, Phys. Rev. B, 68, 155420 (2003).

- [21] I.E.Dzyaloshinskii, E.M.Lifshitz and L.P.Pitaevskii, Adv. Phys., 10, 165 (1961)
- [22] E.V.Theodorovitch, Proc. Roy. Soc. A362 71 (1978).
- [23] L.S. Levitov, Europhys. Lett. 8 499 (1989)
- [24] V.G. Polevoi, Zh. Eksp. Teor. Fiz. 98 1990 (1990).[Sov.Phys. JETP 71 1119 (1990)].
- [25] V.E. Mkrtchian, Phys. Lett. **207** 299 (1995).
- [26] G.V.Dedkov and A.A.Kyasov, Phys.Lett. A **259**, 38, (1999).
- [27] A.A.Kyasov and G.V.Dedkov, Surf.Sci.463, 11 (2000)
- [28] W.L. Schaich and J. Harris, J. Phys. F11 65 (1981).
- [29] J.B. Pendry, J. Phys. C9 10301 (1997).
- [30] B.N.J. Persson and Z. Zhang, Phys.Rev. B 57, 7327 (1998)
- [31] E.M. Lifshitz, Zh. Eksp. Teor. Fiz. 29 94 (1955) [Sov. Phys.-JETP 2 73 (1956)]
- [32] A.I.Volokitin and B.N.J.Persson, Phys. Rev. B 65, 115419 (2002)
- [33] M.S.Tomassone and A.Widom, Phys.Rev. B 56, 4938, (1997).
- [34] E.D.Palik, Handbook of Optical Constants of Solids (Academic, San Diego, CA, 1985)
- [35] L.D.Landau and E.M.Lifshitz, *Statistical Physics*, Pergamon, Oxford, 1970.
- [36] P.Senet, et. al., Chem.Phys.Lett. **299**,389 (1999)
- [37] K.L.Kliever and R.Fuchs, Phys. Rev. 172, 607 (1968); R.Fuchs and K.L.Kliever, Phys. Rev. 186, 905 (1969)
- [38] U. Hartmann, Phys. Rev. B 42, 15441 (1990); 43, 2404 (1991).
- [39] P. Johansson and P. Apell, Phys. Rev. B 56, 4159 (1997).

- [40] J.R.Zurita-Sánchez, J.J.Greffet, L.Novotny, Phys. Rev. B 69, 022902 (2004).
- [41] A.I.Volokitin and B.N.J.Persson, Phys. Rev. Lett. **94**, 086104(2005).





•

